STM JOURNALS

Journal of
Polymer & Composites

ISSN: 2321-2810 (Online)
ISSN: 2321-8525 (Print)
Volume 13, Special Issue 2, 2025
DOI (Journal): 10.37591/JoPC

https://journals.stmjournals.com/jopc

Research JoPC

Modeling of ZnO Based Nano Sensor Device for Evaluating Electronic Interaction with NO_2 Pollutant: Combining Multiphysics Simulation and DFT Study

Indranil Maity[1,*], Aman Kumar Jha[2], Yash Shaw[2]

Abstract

This study focuses on the designing and modeling of a sensor device employing zinc oxide (ZnO) nanowires (NWs), and the evaluation of the chemical response of the same in the presence of nitrogen dioxide (NO_2), which is an acute harmful pollutant for human health and environment. Experimentally synthesized ZnO nanostructures were used as the basis for modeling of the ZnO NWs based sensor device along with a single ZnO NW, utilizing COMSOL Multiphysics (v.4.3). The considered device structure was designed using ZnO NWs array as the central element having two tungsten (W) electrodes. The model was designed on a silicon substrate and ZnO seed layer. Variations in electrical potential and current density were investigated under different voltage inputs. Additionally, Gaussian 09W and GaussView 6.0 were employed to derive the optimized structure of the isolated ZnO NW, along with the calculations of its electronic properties using Density Functional Theory (DFT). A detailed investigation was performed to examine the interaction between nitrogen dioxide (NO_2) gas, and a single ZnO nanowire. The result analysis focused on the details of molecular orbitals (MO) with the lowest unoccupied MO state, the highest occupied MO state and the energy gap between two to evaluate the chemical reactivity and stability of the considered system. Additionally, Electrostatic Potential (ESP) plots were examined to visualize the distribution of electron-dense and electron-depleted areas within the considered structure for understanding of the charge density distribution profile. The findings reveal a notable alteration in the electronic properties of the ZnO nanowire following its interaction with NO_2. This research identifies that ZnO based nanowire's structure can be effectively used as a suitable candidate for NO_2 sensing. The present work not only deepens the understanding of the electronic properties and chemical behaviour of ZnO NW based nano device, but also lays its foundation for diverse applications in chemical/gas sensing, and nanotechnology.

Keywords: ZnO nanowire, COMSOL Multiphysics simulation, gas sensor, nanotechnology, nano-device modeling

***Author for Correspondence**
Indranil Maity

[1]Assistant Professor, Department of Electronics and Communication Engineering (ECE), Institute of Engineering and Management (IEM), University of Engineering & Management (UEM), Kolkata, West Bengal, India
[2]Student, Department of Electronics and Communication Engineering (ECE), Institute of Engineering and Management (IEM), Kolkata, West Bengal, India

Received Date: August 12, 2024
Accepted Date: December 02, 2024
Published Date: January 27, 2025

Citation: Indranil Maity, Aman Kumar Jha, Yash Shaw. Modeling of ZnO based Nano Sensor Device for Evaluating Electronic Interaction with NO_2 Pollutant: Combining Multiphysics Simulation and DFT Study. Journal of Polymer & Composites. 2025; 13(Special Issue 2): S211–S219p.

INTRODUCTION

Gas sensing is crucial as it finds applications in environmental studies, space exploration, agricultural and biomedical domains [1-2]. A thorough investigation has been performed to develop relevant and efficient gas-sensitive materials [3-5]. Low dimensional nanostructured materials have attracted significant interest for their potential in sensing device development. This interest stems from their notable characteristics, including a large surface-to-volume ratio and brilliant chemical and thermal stability across various operating conditions [6-8]. ZnO has garnered significant attention owing to its unique properties, which are attributed to its 3.3 eV wide bandgap and high porosity [9]. It has been

effectively employed in applications like solar cells, biochemical sensors, and elastic electronics [10]. Therefore, gas sensing analysis of ZnO is a topic of current research. ZnO based nanocombs, nanorods, nanotubes, and nano-wires like lower dimensional structures have been experimentally synthesized in particular growth environments [10-12]. Nitrogen dioxide (NO_2) is a notorious air pollutant with severe implications for human health and ecosystems. Chronic exposure to this gas can eventually lead to serious respiratory health risks, like asthma, bronchitis, and a reduction in lung function [13]. NO_2, in particular, can infiltrate deeper into the lungs, causing swelling and increasing the risk of cardiovascular diseases, impaired immune response, and adverse developmental effects in children, including reduced lung growth and cognitive deficits [13-14].

Stiller et al. [15] investigated the electrical resistance of a ZnO nanowire and its variation with temperature (30K–300K) and frequency (40Hz–30MHz). Subanajui et al. investigated carrier transport in metal-nanowire junctions by utilizing ZnO nanowires grown on different substrate configurations [16]. Yong et al. studied ZnO clustered nanowires for its sensitivity and selectivity towards NO and NO_2 for sensing applications, reporting strong effects on their electrical conductivity and magnetic properties [17]. Kumar and colleagues discovered an alteration in the molecular orbital energy gap of ZnO and Ag/ZnO nanorods post adsorption of oxidizing gases such as O_3 and NO_2 [18]. Ali et al. employed spin-polarized DFT to investigate H_2 adsorption by ZnO nanotubes and how defects and dopants affect this property [19]. Several studies have been conducted to examine the electrical properties of ZnO nanostructures, as well as the gas sensing capabilities of ZnO low-dimensional structures. However, few studies have compared electrical parameters like current density distribution, HOMO-LUMO energy gap, and ESP of a single ZnO NW, which is part of a nanodevice, to ascertain selective sensing response of ZnO NW.

The current study aims to develop a novel ZnO NWs-based nano-device in the COMSOL Multiphysics simulation platform using experimentally grown/synthesized ZnO-based nanostructures on a silicon (Si) substrate and a ZnO seed layer as the basis, as reported by Dutta et al. [20]. Instead of a capacitive mode, two tungsten (W) electrodes were used (horizontally) for a resistive mode configuration [4, 6]. Tungsten was chosen for the simulation study due to its high electrical conductivity and reliability. The modeling and simulation of its electronic properties were studied by examining the electric potential and current density. Both the ZnO-based nano-device structure and an individual ZnO nanowire were simulated for varying input bias voltages (0-5 V) applied across W electrodes. The interaction between ZnO nanowires and NO_2 results in the formation of a NO_2 adsorbed nano-composite sensor, enabling the investigation of modified electronic properties like molecular orbitals, HOMO-LUMO energy gap, and ESP.

COMPUTATIONAL METHODS

Figure 1(a-b) depicts the device model's various components. The device structure consists of four major components: (i) a silicon (Si) substrate, (ii) a ZnO seed layer, (iii) ZnO nanowires (ZnO NWs), and (iv) tungsten (W) electrodes. The silicon substrate dimensions are 500 x 500 x 50 nm. It is used to provide mechanical support. The same-sized ZnO seed layer (500 x 500 x 50 nm) over a Si substrate was modelled here to serve as the experimental platform for ZnO NWs. ZnO NWs with a radius of 50 nm and a height of 600 nm were generated using the array setting in the COMSOL Multiphysics software. To allow for thorough analysis, two tungsten electrodes measuring 100 x 300 x 30 nm were positioned symmetrically (horizontally) over the ZnO NWs. As Figure 2 shows, normal meshing was implemented in the device, using the Electric Currents (EC) module. The molecular structure of ZnO nanowire was analyzed computationally using Gaussian 09W and GaussView 6.0. The PM6 method was used for optimization in the ground state during semi-empirical calculations to determine molecular orbitals and conduct ESP analysis.

RESULTS AND DISCUSSION

Study of Electrical Properties of ZnO Based Nanodevice Using COMSOL Simulation

To investigate the variation of electric potential across the ZnO-based nanodevice, an input voltage of 5 V was applied to the right (tungsten) electrode (RE), and 0 V to the left (tungsten) electrode (LE),

as depicted by red and blue colors, respectively in Figure 3. The electric potential was found to be strong just below the electrodes (indicated by dense red and blue colors for RE and LE, respectively). In both cases, the potential gradually varied from top to bottom, beneath the electrode regions—transitioning from red to green (in RE) and from blue to green (in LE). Consequently, as Figure. 3 depicts, the electric potential distribution formed a 'U' shape, when combining the potential distribution was combined according to the color legend bar when observed from left to right electrode i.e., from red to blue. The same analysis was conducted for a single ZnO nanowire located under the right electrode, with the bottom plate of the ZnO NW grounded (blue color).

Figure 4 presents the simulation results, which also aligns with the electric potential distribution observed in the entire device. The variation in current density (CD) for a single ZnO nanowire was examined. For the majority of the NW structure, the CD was uniform (yellow color), as shown in Figure 4. However, some non-uniformity was observed near the top end of the ZnO nanowire (indicated by blue and red lines). At the boundary/interface of any material, the effects of the electric field and electric potential are stronger due to a higher number of defect states. Therefore, when a bias voltage was applied to the top and bottom faces of the ZnO NW, it significantly modulated the localized carrier concentration and mobility. Thus, variations in the current density (CD) are noticeable near the top bias-induced ZnO NW surface.

Study of Molecular Structure and ESP of ZnO NW

After optimization using first-principle calculations, the structure and interaction of ZnO NW with NO_2 gas were analyzed. Figure. 5 depicts the optimized structure of a single ZnO NW. Visualizations of the HOMO and LUMO orbitals, as well as the orbitals just below and above these levels, were evaluated using GaussView 6.0 to study the electronic interaction between the sensing nanowire and the gas molecule. The HOMO-LUMO gap, an important parameter, indicates chemical reactivity and stability; a smaller gap suggests higher reactivity and lower stability, while a larger gap suggests lower reactivity and higher stability [21-23]. The color gradient in HOMO-LUMO plots conveys orbital distribution and intensity, with red and green color representing the positive and negative phases of the molecular orbital wavefunction, respectively [22].

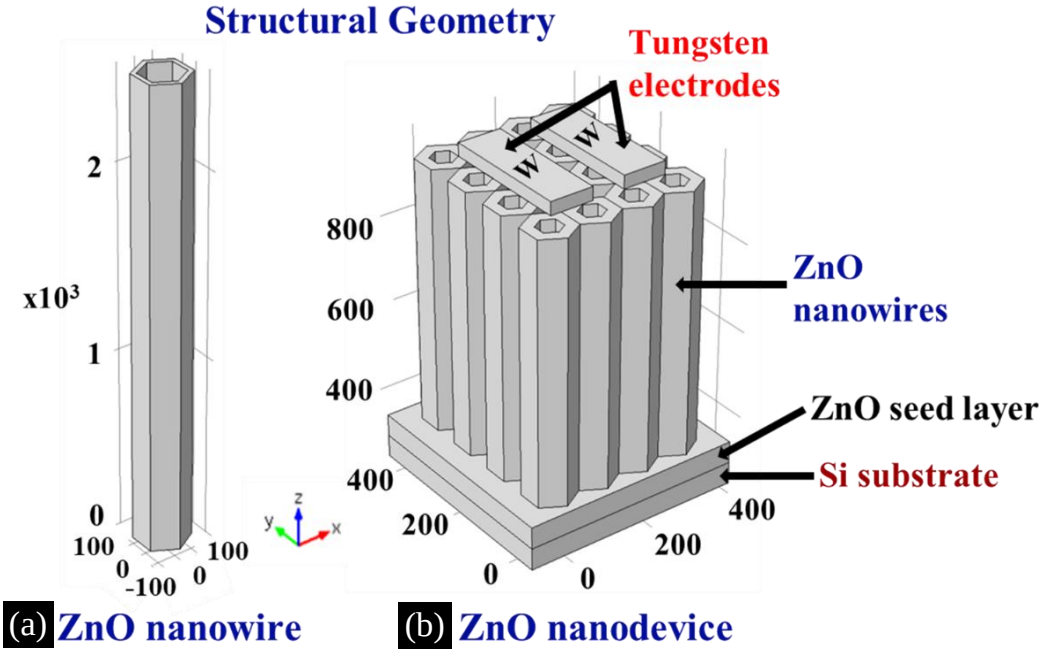

Figure 1. Structural Representation of (a) ZnO Nanowire, and (b) ZnO Nanodevice.

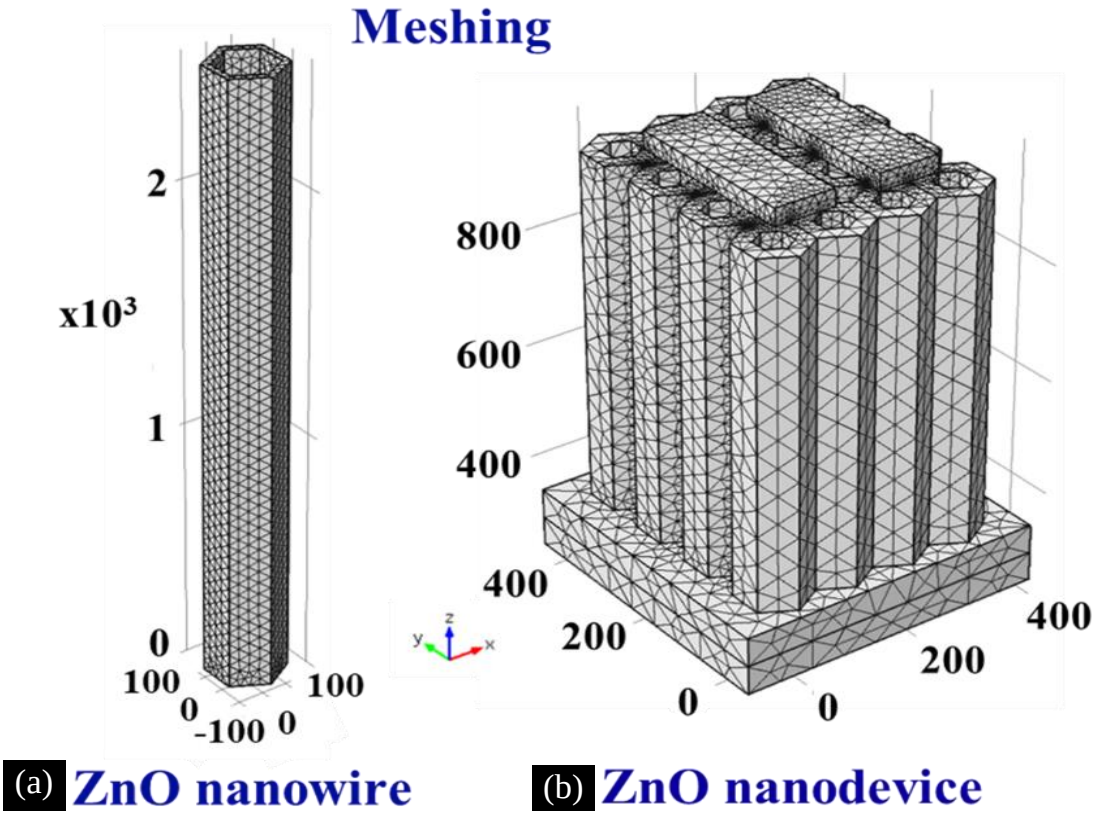

Figure 2. Mesh Representation of (a) ZnO Nanowire, and (b) ZnO Nanodevice.

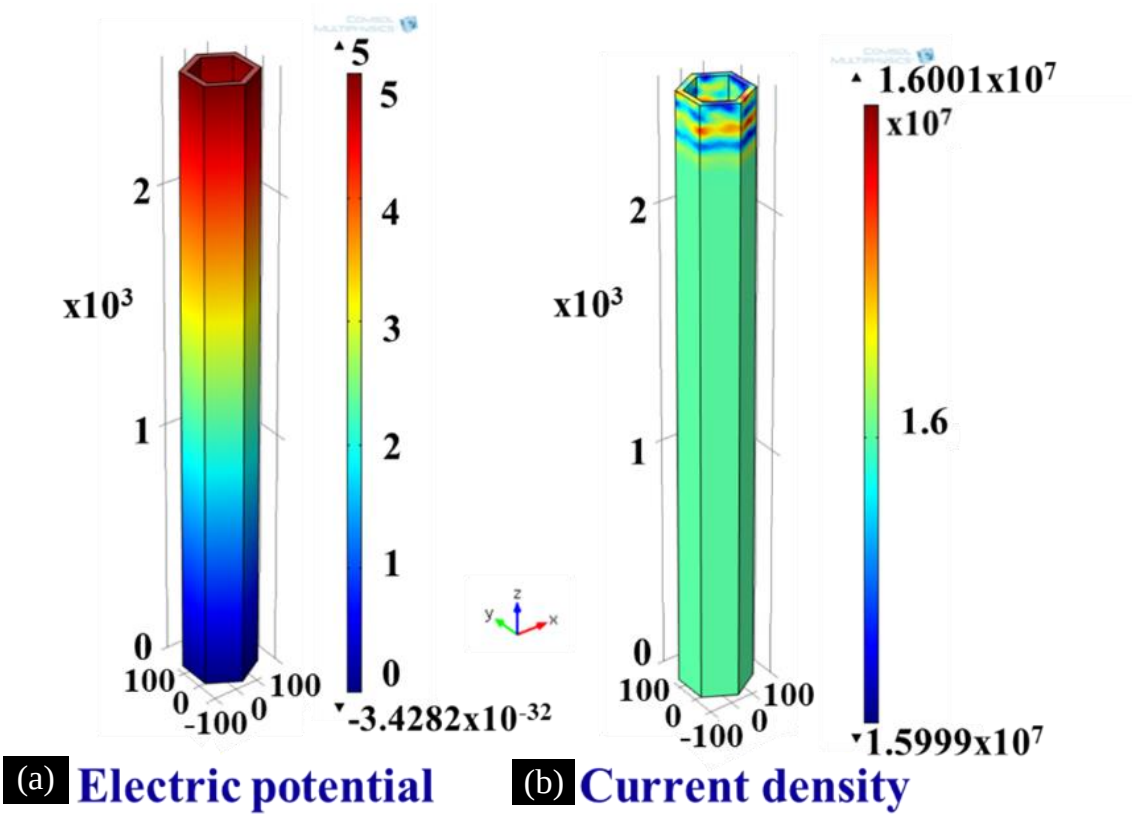

Figure 3. Variation in Single ZnO Nanowire of (a) Electric Potential, and (b) Electric Current Density.

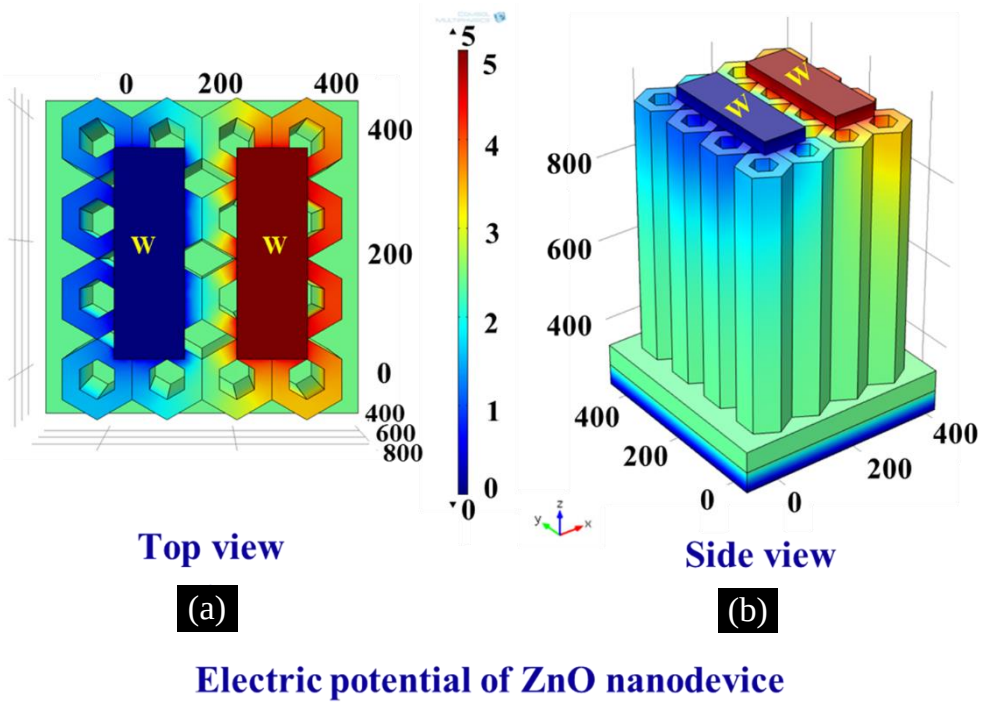

Figure 4. Variation of Electric Potential into Nanodevice Model.

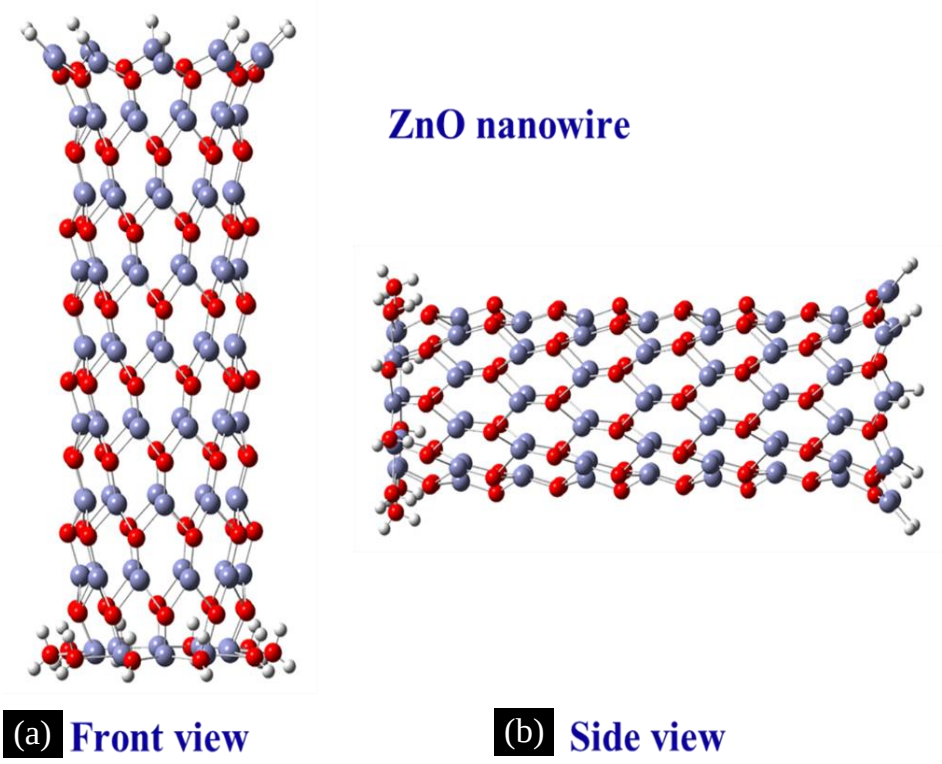

Figure 5. Optimised Structure of Single ZnO Nanowire

Figure 6 displays the molecular orbitals for single ZnO NW with the energy values for all the alpha molecular orbitals and their corresponding energy gap is listed in Table 1. For single ZnO NW, the HOMO-LUMO gap for alpha MO is approximately +2.573 eV with an isovalue of 0.008.

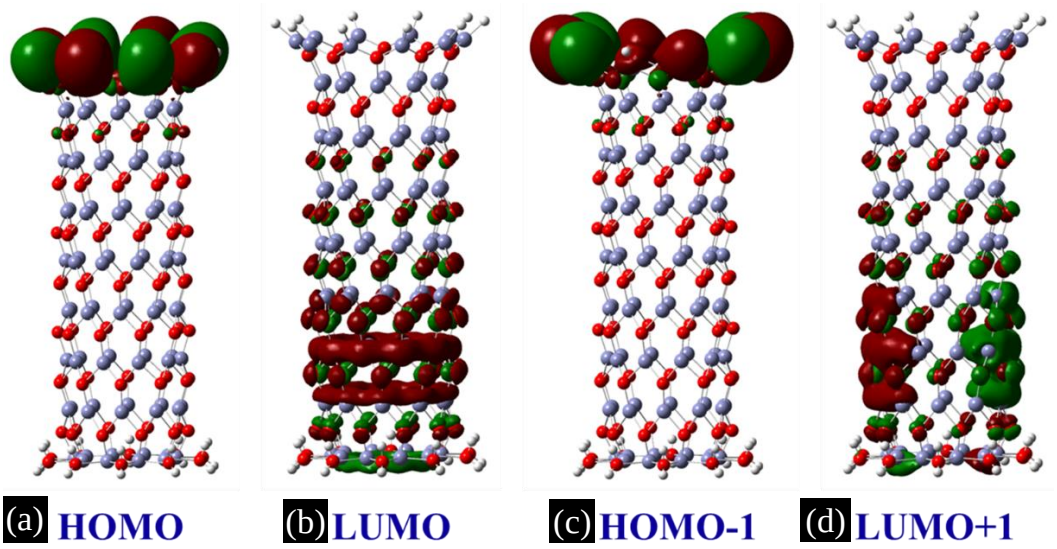

Figure 6. Visual Representation of Molecular Orbitals of ZnO Nanowire.

Table 1. Molecular Orbital Energies of ZnO Nanowire.

Alpha orbitals (in eV)	
E_{HOMO}	-9.005
E_{LUMO}	-6.432
E_{HOMO-1}	-9.005
E_{LUMO+1}	-6.062
$E_{HOMO - LUMO\ gap}$	+2.573
$E_{\{(HOMO-1) - (LUMO+1)\}\ gap}$	+2.943

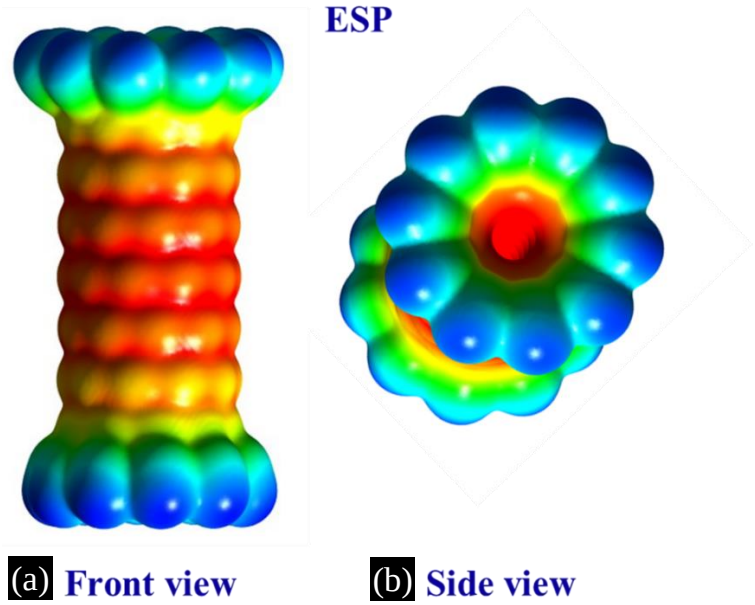

Figure 7. Electrostatic Potential Plot of ZnO Nanowire (a) Front View, and (b) Side View.

Electrostatic Potential (ESP) analysis, generated using GaussView with an isovalue of 0.004, helps to identify reactive sites for electrophilic (red and yellow regions) and nucleophilic (blue regions) attacks [23]. ESP color schemes denote electron-rich (red), electron-deficient (blue), moderately electron-rich (yellow), moderately electron-deficient (cyan), and neutral (green) regions [23-26].

Table 2. Molecular Orbital Energies of NO_2 Adsorbed ZnO Nanowire.

Alpha orbitals (in eV)		Beta orbitals (in eV)	
E_{HOMO}	-9.432	E_{HOMO}	-9.432
E_{LUMO}	-5.777	E_{LUMO}	-5.777
E_{HOMO-1}	-9.691	E_{HOMO-1}	-9.691
E_{LUMO+1}	-5.313	E_{LUMO+1}	-5.313
$E_{HOMO - LUMO\ gap}$	+3.655	$E_{HOMO - LUMO\ gap}$	+3.655
$E_{\{(HOMO-1) - (LUMO+1)\}\ gap}$	+4.378	$E_{\{(HOMO-1) - (LUMO+1)\}\ gap}$	+4.378

Figure 7 depicts the ESP plot for single ZnO NW in a 3D model, highlighting the reactive sites. ESP orientations were shown at two angles in Figure. 7(a-b), with colors ranging from -7.200 e0 eV to -4.300 e0 eV. The isovalue used was 0.0004. Each atom's distinct charge contributes to the ESP distribution.

Study of Molecular Structure and ESP of NO_2 Adsorbed ZnO NW

Figure 8 displays the molecular orbitals for NO_2 adsorbed system, with the energy values and energy gap for the corresponding alpha and beta molecular orbitals is listed in Table 2. For NO_2 adsorption, the HOMO-LUMO gap for alpha MO is approximately +3.655 eV and for beta MO, the value is +3.413 eV.

The ESP plot for the NO_2-adsorbed system is displayed in a 3D model in Figure. 9, highlighting reactive sites. ESP orientations are shown at two angles in Figure. 9(a-b), with colors ranging from -7.255 e0 eV to -3.800 e0 eV. The isovalue used was 0.0004. Post interaction, the strength of red and blue color in ESP weakened as NO_2 is electron withdrawing molecule, thus altering charge density in the ZnO NW. The NW shifts to a more stable state after NO_2 interaction, also evident from the increased HOMO-LUMO energy gap, discussed above.

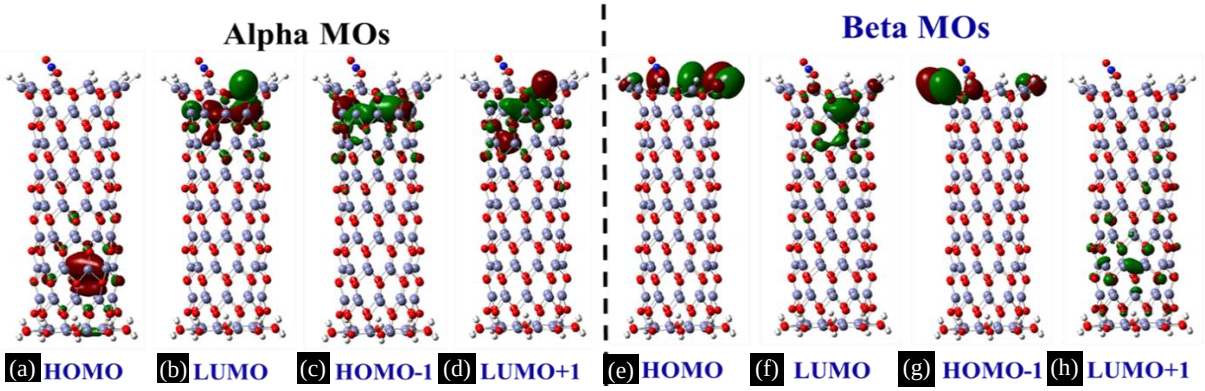

Figure 8. Visual Representation of Alpha and Beta Molecular Orbitals of NO_2 Adsorbed ZnO Nanowire.

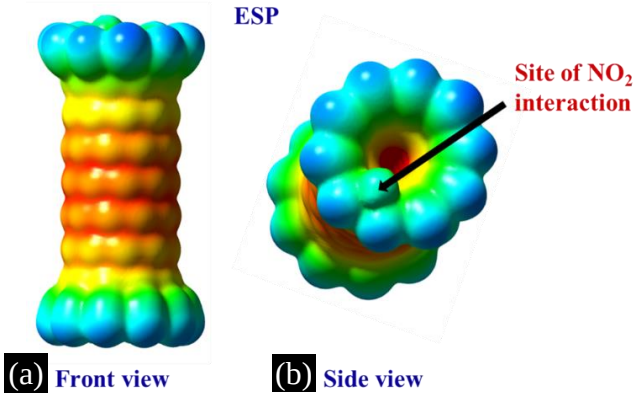

Figure 9. Electrostatic Potential Plot of NO_2 Adsorbed ZnO Nanowire (a) Front View, (b) Side View.

CONCLUSION

This study explored the interaction mechanism between NO_2 gas and ZnO NWs by combining the Multiphysics simulations with DFT calculations performed on the Gaussian platform. Our results indicated that the ZnO NWs exhibited strong interactions with NO_2 molecules, significantly altering its electronic properties. Modulations in electric potential and current density reflect the capability of ZnO NW to detect NO_2 by monitoring crucial parameters of the sensor device. The increased energy gap (by 1.42 times) suggested enhanced stability of the structure during NO_2 adsorption, indicating a shift to a more stable electronic configuration. Furthermore, the electron-rich regions (red) and electron-deficient regions (blue) observed in the ESP plots provide insights into the reactive sites of the ZnO NWs. The weakening of the blue and red regions after NO_2 adsorption indicates a redistribution of electron density, confirming the effective interaction between NO_2 molecules and the ZnO NWs. These changes highlighted the sensor's sensitivity and selectivity, demonstrating ZnO nanowire's effectiveness in detecting NO_2. In conclusion, this study demonstrated that ZnO nanowires are highly sensitive to NO_2 gas due to significant changes in their electronic properties upon gas adsorption. Thus, ZnO NWs can be used as effective gas sensors for detecting NO_2, leading to improvements in environmental monitoring and pollution management technology. This research advances our comprehension of the electronic properties and behavior of ZnO nanowires, providing a strong basis for their use in sensing technologies.

Acknowledgement

The authors would like to thank Siddhartha Bhattacharya, Soubarno Chatterjee and Souvik Bhanja of Department of Electronics and Communication Engineering (ECE) of Institute of Engineering and Management (IEM), Kolkata. The authors also sincerely acknowledge Mr. Indrajit Maity, Department of EE, IIT Bombay for providing support in this research work.

REFERENCES

1. Betty CA, Choudhury S, Shah A. Nanostructured metal oxide semiconductors and composites for reliable trace gas sensing at room temperature. *Surfaces and Interfaces*. 2023 Feb 1; 36:102560.
2. Zhang S, Song P, Wang Q, Ding Y. Ultra-sensitive triethylamine gas sensor based on ZnO/MoO_3 heterostructures with ppb level detection. *Sensors and Actuators B: Chemical*. 2023 Mar 15; 379:133239.
3. Woo HS, Na CW, Lee JH. Design of highly selective gas sensors via physicochemical modification of oxide nanowires: overview. *Sensors*. 2016 Sep 20; 16(9):1531.
4. Saini G, Kumari P, Sharma B.S. Examination of nano-crystalline zinc oxide and zinc oxide doped with aluminum using micro-Raman technology, *RP Current Trends in Applied Science*. 2022; 1: 21–25.
5. Sun K, Zhan G, Zhang L, Wang Z, Lin S. Highly sensitive NO_2 gas sensor based on ZnO nanoarray modulated by oxygen vacancy with Ce doping. *Sensors and Actuators B: Chemical*. 2023 Mar 15; 379:133294.
6. Maity I, Acharyya D, Huang K, Chung P, Ho M, Bhattacharyya P. A comparative study on performance improvement of ZnO nanotubes based alcohol sensor devices by Pd and rGO hybridization. *IEEE Transactions on Electron Devices*. 2018 Jun 29; 65(8):3528-34.
7. Maity I. Cadence Virtuoso based circuit simulation of universal logic gates: A board tutorial. *RP Current Trends in Engineering and Technology*. 2024; 3: 1–7.
8. Acar C, Dincer I, Naterer GF. Review of photocatalytic water-splitting methods for sustainable hydrogen production. *International Journal of Energy Research*. 2016 Sep; 40(11):1449-73.
9. Ansari G, Pal A, Srivastava AK, Verma G. Detection of hemoglobin concentration in human blood samples using a zinc oxide nanowire and graphene layer heterostructure based refractive index biosensor. *Optics & Laser Technology*. 2023 Sep 1; 164:109495.

10. Maity I, Ghosh K, Rahaman H, Bhattacharyya P. Tuning of electronic properties of edge oxidized armchair graphene nanoribbon by the variation of oxygen amounts and positions. *Journal of Materials Science: Materials in Electronics*. 2017 Jun; 28: 9039-47.
11. Prasad B, Bali R. Mathematical study of nanocomposites for drug delivery in capillary. *RP Materials: Proceedings*. 2023; 2(1): 1–10.
12. Kumari M. Micro-Raman investigation of nano-crystalline ZnO and ZnO doped with Al, *RP Current Trends in Engineering and Technology*. 2022; 1: 57–61.
13. Guo LY, Xia SY, Sun H, Li CH, Long Y, Zhu C, Gui Y, Huang Z, Li J. A DFT study of the Ag-doped h-BN monolayer for harmful gases (NO_2, SO_2F_2, and NO). *Surfaces and Interfaces*. 2022 Aug 1; 32:102113.
14. Zhao S, Liu S, Sun Y, Liu Y, Beazley R, Hou X. Assessing NO_2-related health effects by non-linear and linear methods on a national level. *Science of the Total Environment*. 2020 Nov 20; 744:140909.
15. Stiller M, Barzola-Quiquia J, Zoraghi M, Esquinazi P. Electrical properties of ZnO single nanowires. *Nanotechnology*. 2015 Sep 11; 26(39): 395703.
16. Subannajui K, Kim DS, Zacharias M. Electrical analysis of individual ZnO nanowires. *Journal of Applied Physics*. 2008 Jul 1; 104(1).
17. Yong Y, Su X, Zhou Q, Kuang Y, Li X. The $Zn_{12}O_{12}$ cluster-assembled nanowires as a highly sensitive and selective gas sensor for NO and NO_2. *Scientific reports*. 2017 Dec 13; 7(1): 17505.
18. Kumar U, Huang SM, Deng ZY, Yang CX, Haung WM, Wu CH. Comparative DFT dual gas adsorption model of ZnO and Ag/ZnO with experimental applications as gas detection at ppb level. *Nanotechnology*. 2021 Dec 16; 33(10):105502.
19. Ali M, Tit N, Yamani ZH. Role of defects and dopants in zinc oxide nanotubes for gas sensing and energy storage applications. *International Journal of Energy Research*. 2020 Oct 25; 44(13):10926-36.
20. Dutta K, Banerjee N, Mishra H, Bhattacharyya P. Performance improvement of Pd/ZnO-NR/Si MIS gas sensor device in capacitive mode: Correlation with equivalent-circuit elements. *IEEE Transactions on Electron Devices*. 2016 Feb 8; 63(3):1266-73.
21. Maity I, Ghosh K, Rahaman H, Bhattacharyya P. Selectivity tuning of graphene oxide based reliable gas sensor devices by tailoring the oxygen functional groups: A DFT study based approach. *IEEE Transactions on Device and Materials Reliability*. 2017 Oct 25; 17(4):738-45.
22. Singh JS, Khan MS, Uddin S. A DFT study of vibrational spectra of 5-chlorouracil with molecular structure, HOMO–LUMO, MEPs/ESPs and thermodynamic properties. *Polymer Bulletin*. 2023 Mar; 80(3):3055-83.
23. Maity I, Bhattacharyya P. Room temperature acetone sensing performance of rGO-ZnO nanotubes binary hybrid structure. *Sensor Letters*. 2019 Jun 1; 17(6):417-22.
24. Mahmood A, Akram T, de Lima EB. Syntheses, spectroscopic investigation and electronic properties of two sulfonamide derivatives: a combined experimental and quantum chemical approach. *Journal of Molecular Structure*. 2016 Mar 15; 1108:496-507.
25. Chen Y, Gui Y, Chen X. Adsorption and gas-sensing properties of C_2H_4, CH_4, H_2, H_2O on metal oxides (CuO, NiO) modified SnS_2 monolayer: A DFT study. *Results in Physics*. 2021 Sep 1; 28:104680.
26. Maity I, Nagasawa H, Tsuru T, Bhattacharyya P. Correlation between ammonia selectivity and temperature dependent functional group tuning of GO. *IEEE Transactions on Nanotechnology*. 2020 Dec 18; 20:129-36.

